Biology of Reproduction, 2024, **111(4)**, 959–974
https://doi.org/10.1093/biolre/ioae115
Advance access publication date 30 July 2024
Research Article

Temporal maturation of Sertoli cells during the establishment of the cycle of the seminiferous epithelium†

Shelby L. Havel and Michael D. Griswold*

School of Molecular Biosciences, Washington State University, Pullman, WA 99164, USA

***Correspondence:** Michael D. Griswold, BLS 202 100 Dairy Road Pullman, WA 99164, USA. E-mail: mgriswold@wsu.edu

†**Grant Support:** Federal funding provided by NIH grant R01 HD10808 awarded to Michael D. Griswold.

Abstract

Sertoli cells, omnipresent, somatic cells within the seminiferous tubules of the mammalian testis are essential to male fertility. Sertoli cells maintain the integrity of the testicular microenvironment, regulate hormone synthesis, and of particular importance, synthesize the active derivative of vitamin A, *all trans* retinoic acid (*at*RA), which is required for germ cell differentiation and the commitment of male germ cells to meiosis. Stages VIII–IX, when *at*RA synthesis occurs in the testis, coincide with multiple germ cell development and testicular restructuring events that rely on Sertoli cell gene products to proceed normally. In this study, we have synchronized and captured the mouse testis at four recurrent points of *at*RA synthesis to observe transcriptomic changes within Sertoli cells as mice age and the Sertoli cells are exposed to increasingly developed germ cell subtypes. This work provides comprehensive, high-resolution characterization of the timing of induction of functional Sertoli cell genes across the first wave of spermatogenesis, and outlines in silico predictions of germ cell derived signaling mechanisms targeting Sertoli cells. We have found that Sertoli cells adapt to their environment, especially to the needs of the germ cell populations present and establish germ-Sertoli cell and Sertoli-Sertoli cell junctions early but gain many of their known immune-regulatory and protein secretory functions in preparation for spermiogenesis and spermiation. Additionally, we have found unique patterns of germ-Sertoli signaling present at each endogenous pulse of *at*RA, suggesting individual functions of the various germ cells in germ-Sertoli communication.

Summary Sentence
Stages VIII–IX of the cycle of the seminiferous epithelium are of critical importance to the successful continuation of sperm production, and this work characterizes (i) the induction of known functional Sertoli cell genes at each successive occurrence of stages VIII–IX, and (ii) the predicted cell signaling pathways that target Sertoli cells and originate from various germ cell subtypes produced across the first round of spermatogenesis.

Graphical Abstract

Created with Biorender.com

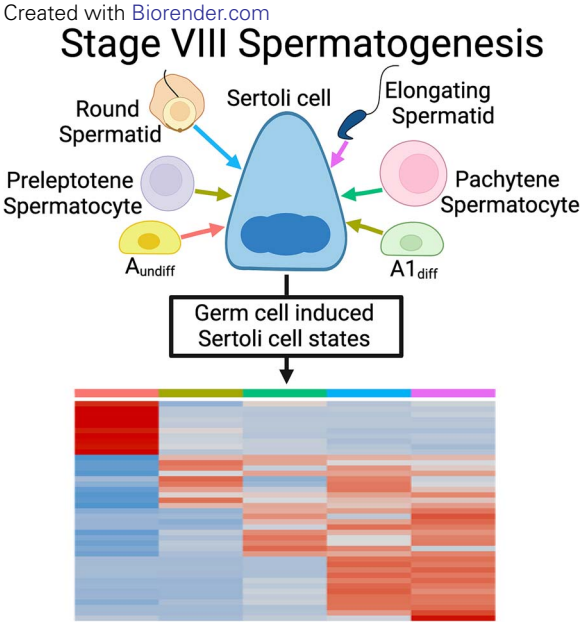

Key words: Sertoli cell, spermatogenesis, single cell RNA-sequencing, maturation, signaling, retinoic acid

Received: February 28, 2024. **Revised:** June 5, 2024. **Accepted:** July 29, 2024

Introduction

Currently, infertility, defined as more than a year's time of attempting to conceive a child without success [1], is being increasingly attributed to the male partner. A male derived defect has been found to contribute to more than half of all diagnosed cases of infertility; however, many of these cases are without a direct or identifiable cause [2, 3].

To unravel the causes of male infertility, it is critically important to understand what drives the process of spermatogenesis forward. Spermatogenesis is the process by which all male germ cells are produced and, in the mouse, this occurs across 12 distinct "stages" marked by the specific appearance of various germ cell subtypes and the cellular associations they form within the seminiferous tubules of the testes. Spermatogenesis occurs in a cyclic, asynchronous manner and the continual appearance of the 12 stages is referred to as the cycle of the seminiferous epithelium [4, 5]. Spermatogenesis begins at ~3–5 days post-partum (DPP) in the mouse, and four complete cycles of the seminiferous epithelium are required before mature, elongated spermatids are produced and released from the seminiferous tubules [6]. This process takes ~35 days in the mouse, with each cycle lasting ~8.6 days. The exception to this rule is the first cycle, which is shorter and requires only ~6 days to complete [7, 8].

Sertoli cells, often referred to as "nurse cells" within the tubules, are essential to the progression of spermatogenesis and carry out many tasks that both (i) support the germ cells as they develop and (ii) the overall health of the testicular microenvironment [9–12]. Sertoli cells form tight junctions between themselves to form the blood-testis-barrier (BTB) that protects the germ cells from being targeted by the immune system, and aids in dividing the tubule interior into a basal and adluminal compartment. This compartmentalization provides distinct environmental stimulus to the various germ cells produced as they progress through spermatogenesis [9, 13, 14]. They also secrete many classes of proteins which range wildly in function. Some of these proteins include metal ion transporters, regulators of hormones such as follicle stimulating hormone and testosterone, proteases important for testicular remodeling and sperm release, and controllers of the immune response [10–12, 15–17].

Arguably, however, the most important function of Sertoli cells is the synthesis of *all-trans* retinoic acid (*at*RA). Testicular *at*RA synthesis occurs cyclically (in the mouse) peaking in stages VIII and IX [18]. Stages VIII–IX of the murine cycle of the seminiferous epithelium are of critical importance and directly coincide with several major spermatogenic events. The first is the irreversible commitment of the A undifferentiated spermatogonia (A_{undiff}) progenitor cells, which are produced by spermatogonial stem cells, to differentiation. This is initiated by *at*RA exposure, and the A_{undiff} cells transition into A1 differentiating spermatogonia ($A1_{diff}$). The second is meiotic initiation in spermatocytes, and the third is spermiation, the release of elongated spermatids into the lumen space of the seminiferous tubule [6, 18]. The commitment of A_{undiff} population to $A1_{diff}$ cells, has been referred to as the "A to A1 transition" and without this step, or the *at*RA synthesized by Sertoli cells, spermatogenesis cannot proceed [19–21].

Recent findings have emphasized the importance of germ cells on the normal function of Sertoli cells. Using single cell RNA sequencing (scRNA-seq), adult Sertoli cells were divided into nine sub-groups based on gene expression data [22]. Later, scRNA-seq on Sertoli cells isolated from adult mice observed similar diversity in the captured cell population, condensed this heterogeneity into two defined groups using hierarchical clustering [23]. These two groups of Sertoli cells isolated from an adult mouse testis defined two separate transcriptional states: one that occurs during stages VIII–IX, and one encompassing all the remaining stages (X–VI). During the stages VIII–IX there was a major induction of differentially expressed genes from both Sertoli cells and germ cells [23]. Abolishing the germ cell population using a genetic knockout model, however, eliminated any differential gene expression across the entire cycle of the seminiferous epithelium. This result confirmed the long-held concept that there must be signaling between germ and Sertoli cells that are critical for maintaining normal Sertoli cell populations, function, and the regular progression of spermatogenesis overall [23]. What these signals may be, which germ cell subtypes are sending them, and when, however, is still largely unknown.

Cellular events in stages VIII–IX of the cycle are essential for successful and continuing spermatogenesis in the mouse. The commitment of A_{undiff} spermatogonia to differentiation, the dynamics of the tight junction formation, and the release of fully formed spermatids occur at these stages because of the synthesis and actions of *at*RA [6, 18, 24]. Each of these processes is perhaps dependent on the interactions between Sertoli cells and germ cells and the result is transcriptional changes in both cell types [23]. The specificity of the interactions between developing Sertoli cells and the different germ cell populations is unknown, so we utilized WIN 18 446 to synchronize spermatogenesis in the testis and were able to determine changes in transcriptional response of both cell types at each occurrence of stages VIII to IX from the original RA pulse to spermiation [25–27]. WIN 18 446 is a previously identified inhibitor of aldehyde dehydrogenase enzymes, which are essential to the synthesis of *at*RA [27]. Daily treatment with WIN 18 446 results in a block in spermatogenesis as a result of failed clearance of the transition of A_{undiff} cells to differentiation, which can be released following IP-injection with exogenous *at*RA, resulting in synchronized spermatogenic progression with the entire testis being made up of only approximately three to five stages at a given time, although normal spermatogenic timing is maintained [20, 26].

In this work, we performed scRNA-seq on whole testis samples isolated from wild-type C57BL/6 J mice following treatment with WIN 18 446 and exogenous *at*RA. This method has allowed us to capture transcriptional information from all cells from stages VIII–IX of spermatogenesis with high specificity during each of the four cycles that occur prior to spermiation. The primary goal of this work was to obtain information on differential gene expression in Sertoli cells as well as signaling mechanisms occurring between the various germ cell subtypes and Sertoli cells during stage VIII–IX of spermatogenesis.

Methods

Animal husbandry

All work performed with animals was approved by the Washington State University Animal Care and Use Committees and were accordance with the principles for the care and use of research animals for the National Institutes of Health under Animal Subject Approval Form (ASAF)

#6452 at the Washington State University Pullman campus. Wild-type C57BL/6 J males (Jackson Laboratory, Bar Harbor, ME, USA) were used for scRNA-seq analysis and histology. Animals expressing the RFP construct (B6.Cg-*Gt(ROSA)26Sor*$^{tm14(CAG-tdTomato)Hze}$/J; Jackson Laboratory, Bar Harbor, ME, USA) were bred with AMH-Cre possessing animals (C57BL/6 J) [28] to produce a colony of AMH-Cre^{+};RFP$^{fl/fl}$ homozygous progeny that were used for fluorescently activated cell sorted (FACS). Animals were housed in a humidity- and temperature-controlled environment with food and water provided ad libitum. At the time of tissue collection, mice were euthanized via carbon dioxide asphyxiation followed by either decapitation (if the animal was younger than 21DPP) or cervical dislocation (if the animal was 21DPP and older).

Mouse genotyping

AMH-Cre^{+};RFP$^{fl/fl}$ experimental mice were tested for the presence of the floxed RFP construct and AMH-Cre transgene by collecting, digesting, and performing PCR on tail cuts as previously reported [23]. The RFP wild-type band is present at 397 bp, and the RFP-floxed band is at 196 bp. The Amh-Cre wild-type band is at 180 bp, and the AMH-Cre-positive band is at 100 bp. The primers used for detection of the RFP construct (WT forward 5′-AAG GAG CTG CAG TGG ACT A-3′, WT reverse 5′-CCG AAA ATC TGT GGG AAG T-3′, RFP forward 5′-CTG TTC CTG TAC GGC ATG G-3′, RFP reverse 5′-GGC ATT AAA GCA GCG TAT CC-3′) and the primers used for detection of the AMH-Cre transgene (WT forward 5′-CTA TCG TGG ATC AGC GAC CTT C-3′, WT reverse 5′-CAC GGG AAC GAA ATG AAC ACC-3′, AMH-Cre forward 5′-GCG GTC TGG CAG TAA AAA CTA TC-3′, AMH-Cre reverse 5′-GTGAAA CAG CAT TGC TGT CAC TT-3′) are listed here and have been published in previous work [23]. RFP mice were previously purchased from the Jackson Laboratory, Bar Harbor, ME, USA (stock no. 007914) and AMH-Cre mice were a gift from Marie-Claude Hofmann [28].

BDAD synchrony/RA injections

Spermatogenesis synchronization was performed as previously described [20, 23, 25, 26]. Control animals were euthanized without receiving an injection of exogenous *at*RA following 7 days of WIN 18 446 treatment at 9DPP. Animals collected for further timepoints were aged out between six and 40.2 days post 100 mg/kg daily WIN 18 446 treatment and 200 μg *at*RA injection as described prior to euthanasia (Fig. 1A). From the C57BL/6 J animals, one testis was used to generate a single cell suspension. The other testis was placed in Bouin's fixative (71% saturated picric acid [21 g/L], 24% formaldehyde, 5% glacial acetic acid) for 3 h at room temperature (if the animal was younger than 30DPP) or six hours at room temperature (if the animal was older than 30DPP) prior to processing/embedding.

Histology and staging

After fixation, the testes were taken through a graded series of ethanol washes before clearing with xylenes, then tissue was embedded in paraffin wax prior to being sectioned at 5 μM thick on Superfrost Plus slides (ThermoFisher, Waltham, MA, USA) for subsequent histology. Sections were stained with hematoxylin and eosin as previously described [21]. Stages were then determined via characterization of the mouse seminiferous epithelium [4, 29, 30]. We have previously asserted that synchrony remains consistent with approximately five stages present per animal [20, 23, 26], and this was supported by our presented findings. A minimum of three separate testes pairs were used for analysis, with a minimum of 200 tubule cross sections collected for each timepoint. Replicates of each testis were cut at least 50 microns apart. Data are presented as averages +/− standard deviation (SD).

Single cell suspensions

To create a single cell suspension, testes were detunicated and dissociated as was previously described [23]. Cell counts were estimated using a hemocytometer, spun down at 600 × *g* for 7 min at 4°C, and resuspended at 4 million cells/mL in 10% DNase in 1x DPBS (ThermoFisher, Waltham, MA, USA). To determine cell viability, 20 μL of the cell suspension was diluted 1:1 with 0.4% trypan blue (Invitrogen, Waltham, MA, USA), and on average the cell suspensions used for scRNA-seq library had a live cell percentage of at least 96.95% (+/− 2.52%). Total time from tissue dissociation to library preparation was ∼90 min, and all libraries were produced immediately following single cell suspension prep. Data are presented as averages +/− standard deviation (SD).

scRNA-seq library prep and sequencing

Cells from triplicate males (n = 3) were pooled at equal proportions and loaded into a Chromium Controller (10× Genomics, Inc., Pleasanton, CA, USA). Single-cell cDNA libraries were generated using v3.1 chemistry according to the manufacturers protocol (10× Genomics, Inc.) and sequenced via NovaSeq PE150 (Novagene, Sacramento, California) on an Illumina Novaseq 6000 (Novagene, Sacramento, California). Raw data were processed, demultiplexed, and aligned to the 10-mm mouse transcriptome using the 10× Genomics Cell Ranger pipeline (v3.0.2) [31].

After raw data processing, the resulting gene-cell matrix was analyzed further in R software using the Seurat package (v4.3.0.1) [32]. Transcriptomes were excluded if the percent of reads mapping to the mitochondrial genome was greater than 25%. Doublets were identified and excluded from analysis using the package DoubletFinder (v2.0.3) [33]. Gene expression data were then normalized, scaled, and variable genes identified using the default parameters in Seurat. Dimensional reduction was then performed via principal component (PC) analysis and the number of PCs was selected by identifying the point at which the percent change in variation between the consecutive PCs was less than 0.1%, and then corroborated by determining statistical significance ($P > 0.05$) using the "JackStraw" procedure. Individual cells were projected onto uniform manifold approximation projection (UMAP) two-dimensional representations using the selected PCs. Graph-based clustering was performed via Louvain algorithm with the "FindClusters" function (resolution = 0.8). Cell identity was determined by marker gene analysis [23, 34–39]. Sertoli cells were identified using *Sox9, Amh, Aard, Clu, Rhox5,* and *Rhox8*. Germ cells were broadly identified with *Ddx4 and Dazl*, before further division by type. A_{undiff} cells were identified as being *Zbtb16+/Stra8-*. $A1_{diff}$ cells were identified as being positive for *Stra8* and *Ccnd2* whereas preleptotene spermatocytes were identified by being positive for *Stra8* and *Dmc1* but not expressing *Ccnd2-*. Pachytene spermatocytes were identified using the markers *Meiob, Sycp3, Psma8,* and

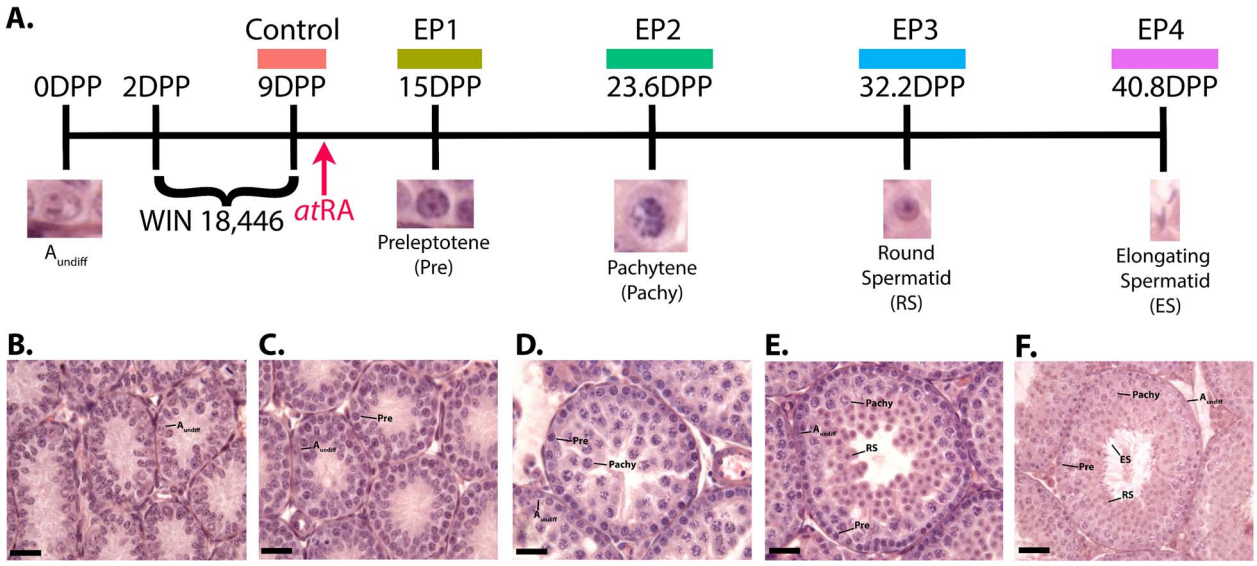

Figure 1. (A) Diagram representing the timing of WIN 18,446 treatment beginning at 2DPP and continuing until 9DPP. Control animals were euthanized at 9DPP, whereas all other experimental animals were injected at 9DPP with *at*RA and then collected at the ages listed for each respective endogenous pulse 1–4 (EP1-EP4). Magnified images of the major germ cell types that emerge at each endogenous pulse are shown beneath the timeline, and all timepoints contain each cell type mentioned previously on the timeline to their collected date. Germ cell types include A_{undiff}, preleptotene spermatocytes (Pre), pachytene spermatocytes (Pachy), step-8 round spermatids (RS), and step-16 elongated spermatids. (B-F) Representative images of seminiferous tubule cross-sections from each sample which show the cellular composition contained within (B) control sample tubules that received no *at*RA injection; (D) EP1 testes; (E) EP2 testes; (F) EP3 testes; (G) and EP4 testes. Each sample has been annotated with labels for characteristic stage VIII germ cell types present (A_{undiff}, Pre, Pachy, RS, and ES). For all histology, a minimum of three separate testes pairs (n = 3) were used for analysis. Replicates of each testis were cut at least 50 microns apart. Scale bars represent 25 μm.

Piwil1. Step-8 round spermatids were identified using the markers *Ccna1*, *Tex36*, *Sun5*, *Prm1*, *Cstl1*, *and Klf4*. Step-16 elongating spermatids were identified using the markers *Prm2*, *Prm3*, *Izumo2*, *Tssk6*, *Dnajb3*, *Spem1*, *Hook1*, *Lamc3*, and *Camk4* Myoid cells were identified with *Cald1*, *Acta2*, and *Myl9*. Endothelial cells were identified with *Sparcl1*. Macrophages were identified with *Lyz2*. Leydig cells were identified with *Cyp17a1*, *Insl3*, and *Lcn2*.

To further analyze Sertoli cells, the identified Sertoli cell populations were subset from the main population of cells and the default Seurat processing steps were repeated, including normalization, scaling, variable gene identification, dimensional reduction, and clustering (resolution = 0.8). In silico isolation was performed by evaluating the isolated Sertoli cell clusters and one resulting cluster was excluded due to germ cell contamination as identified by *Ddx4* and *Dazl* marker gene expression. Genes differentially expressed between each timepoint and the control sample was calculated with "FindAllMarkers" (min.pct = 0.1) and our focus was then narrowed to positive differentially expressed genes with a log fold-change difference ≥ 0.25 and an adjusted p-value <0.05 and a log-fold change difference ≤ -0.25 and an adjusted p-value <0.05 for negative differentially expressed genes.

To evaluate predicted signaling mechanisms present between Sertoli and germ cells at each timepoint, each germ cell population was subset and the default Seurat processing steps were repeated as above for the Sertoli cells. The resulting objects containing the germ and Sertoli cells were merged, and the package CellChat (v1.6.1) [40] was used with "min.cells = 1", "trim = 0.1", and "population.size = FALSE" to not bias the results against the smaller populations of Sertoli cells captured in later timepoints. Only results with a p-value <0.05 were included in analysis.

Cell sorting

Cell sorting was performed on AMH-Cre^{+};RFP$^{fl/fl}$ animals to collect RFP-positive Sertoli cells for AmpliSeq (n = 3 each timepoint). FACS was performed with an SH800 machine (Sony Biotechnology, San Jose, CA, USA) to obtain RFP-positive Sertoli cells following the dissociation and suspension as previously performed [23]. A minimum of 250 000 cells were collected from each animal, before being spun down post-sorting at $600 \times g$ for 7 min at 4°C. The supernatant was removed and all cells were resuspended in 100 μL Trizol (Invitrogen, Waltham, MA, USA) and stored at −20°C until RNA isolation. A representative image depicting the gating strategy used can be seen in Supplementary Fig. S1.

RNA isolation

To isolate total RNA, the Trizol RNA isolation procedure was followed according to the manufacturer's instructions as reported previously [23]. Resulting RNA pellets were resuspended in 25 μL warm nuclease-free water and stored at −80°C until further use.

AmpliSeq analysis

A minimum of 250 000 fluorescently labeled cells were isolated from individual AMH-Cre^{+};RFP$^{fl/fl}$ testes (n = 3) via cell sorting, then total RNA was extracted and pooled at equal concentrations in triplicate before libraries were made using the Ion AmpliSeq Transcriptome Mouse Gene Expression library kit (Ion Torrent, Waltham, MA, USA) and sequencing beads were made using an Ion Chef (Life Technologies, Carlsbad, CA, USA). Samples were run on an Ion GS S5 with Ion 540v1 chips and then analysis was performed using Torrent Suite V5.16.1.

Results

scRNA-seq allows for high resolution analysis of synchronized spermatogenesis

scRNA-seq was performed on animals that were treated with WIN 18 446 beginning at 2DPP and treatment was maintained for 7 days. No *at*RA was given to the control group that were collected at 9DPP, but all other sample groups received an injection of *at*RA at 9DPP. After *at*RA was provided, testes were collected following *at*RA treatment to capture each of the four endogenous pulses of *at*RA, coinciding with stages VIII–IX, prior to spermatid release during spermiation (Fig. 1A). These timepoints will be referred to as the "endogenous pulse of *at*RA 1, 2, 3 and 4" (EP1, EP2, EP3, and EP4), respectively, for the remainder of this work.

Staging performed on each time point verified the effectiveness of the WIN 18 446 treatment. Each sample collected consisted primarily of stage VII–X tubules, with an average of 84.00% (+/− 2.45%) of all the tubules sampled being specific to stages VIII–IX (see Supplemental Fig. S2). The majority of the tubules at each timepoint were captured at stage VIII, which alone comprised an average of 74.86% (+/− 5.94%) of all tubules across the four collected timepoints (see Supplemental Fig. S2) [20, 23, 26]. The control samples represented a testicular state wherein there are only A_{undiff} and Sertoli cells within the seminiferous tubules (Fig. 1B), and each timepoint after represented the first occurrence of new germ cell subtypes. The preleptotene spermatocytes are newly present within the EP1 samples (Fig. 1C), pachytene spermatocytes have formed at EP2 (Fig. 1D), step-8 round spermatids (round spermatids) at EP3 (Fig. 1E), and step-16 elongating spermatids (elongating spermatids) at EP4 (Fig. 1F). $A1_{diff}$ cells are additionally prevalent in each post-*at*RA sample and develop immediately following *at*RA treatment.

Freshly isolated whole testes obtained from three animals at each time point were dissociated, pooled, and underwent scRNA-seq analysis [32]. From these cells, 11 distinct cell types could be discerned (Fig. 2A). These cell assignments are specific as indicated by marker gene analysis (Fig. 2B) and across all the timepoints collected, 40 135 cells remained for analysis across our timepoints (Fig. 2C) [23, 34–39]. Differentially expressed genes (DEGs) for each timepoint against the control sample were identified, and lists of DEGs that are up- and downregulated within Sertoli cells captured at each timepoint have been made available (see Supplemental File S1). To further validate our scRNA-seq data, we performed AmpliSeq on FACS Sertoli cells at each timepoint, and these results were used as supporting data to further characterize the Sertoli cell transcriptome [41].

Close evaluation of the coordinates of each Sertoli cell cluster within the produced UMAP showed that a dramatic shift occurred at EP1 when compared to the control samples following *at*RA treatment (Fig. 2A). This shift is exacerbated when the Sertoli cells were subset from the larger population (Fig. 3A). Hierarchical clustering additionally showed that the heterogeneity present within the timepoints collected was largely due to gene expression differences that emerge following *at*RA treatment, as seen by the immediate separation of the control and all post-*at*RA samples in the clustering dendrogram provided (Fig. 3B).

Analysis of the top 50 DEGs at each time point (Fig. 3C) reiterated this separation and confirmed that our dataset could be divided into two primary groups where our control is separate from all *at*RA treated samples. Comparisons between EP1 derived Sertoli cells compared to Sertoli cells isolated from our control sample revealed downregulation of the immature Sertoli cell marker anti-Mullerian hormone (*Amh*), the upregulation of mature Sertoli cell markers including SRY-box transcription factor 9 (*Sox9*), Wilms tumor protein (*Wt1*), and GATA binding protein 1 (*Gata1*), as well as the induction of follistatin-like ligand 3 (*Fstl3*), a known silencer of Sertoli cell proliferation (Fig. 3D-H).

These data showed that we successfully captured the pre- and post-pubertal state of the testis, which has allowed us to accurately determine when known Sertoli cell expressed genes are induced in each of the post-*at*RA samples, and which genes showed expression prior to the initiation of spermatogenesis coinciding with *at*RA exposure.

Sertoli cell establishment of the BTB and germ-Sertoli cell junctions at stages VIII–IX

Essential to the germ cells' continued development and meiotic progression is the Sertoli cell facilitated establishment, and movement, of preleptotene spermatocytes across the BTB. The BTB is established by tight junctions formed between neighboring Sertoli cells, and we evaluated the expression levels of known tight junction regulating genes, as well as other genes known to regulate Sertoli-germ adhesion junctions including: claudin-11 (*Cldn11*), cingulin (*Cgn*), junctional adhesion molecule 3 (*Jam3*), AT-enriched domain 4a (*Arid4a*), claudin-3 (*Cldn3*), N-cadherin (*Cdh2*), AT-enriched domain 4b (*Arid4b*), tight junctional protein 1 (*Tjp1*) [9] cadherin 23 (*Cdh23*), Cell Division Cycle 42 (*Cdc42*), effector proteins of *Cdc42* (*Cdc42ep5*, *Cdc42ep3*, *Cdc42bpb*, and *Cdc42se2*) [42, 43], and the testicular gap junction protein connexin 43 (*Gja1*) [44].

Sertoli cells isolated at EP1 showed the first expression of *Cldn11*, *Cgn*, and *Jam3*. *Cldn11* expression persisted at all timepoints, where *Cgn* and *Jam3* expression only remained upregulated in the EP1, EP2, and EP3 samples (Fig. 4A-C). Additionally upregulated at this time was *Arid4a*, and the upregulation of *Arid4a* remained consistent throughout all of the post-*at*RA samples (Fig. 4D). *Cldn3* and *Cdh2* were first upregulated within the EP2 Sertoli cells (Fig. 4E/F). *Arid4b* was also upregulated at this time and remained differentially upregulated within Sertoli cells isolated from our EP3 sample (Fig. 4G). Within EP3-isolated Sertoli cells, *Tjp1* and *Cdh23* were differentially upregulated compared to the control sample (Fig. 4H/I).

Cdc42 showed ample mRNA expression within our scRNA-seq data at all timepoints, including within our control samples, as such it was not found to be differentially regulated within any of our collected timepoints (Fig. 4J). However, we found many genes that encode effector proteins of *Cdc42* with mRNA transcript levels that were differentially expressed across the cycle of the seminiferous epithelium. *Cdc42ep5* was upregulated in EP1-EP3 isolated Sertoli cells, *Cdc42ep3* was upregulated only within Sertoli cells isolated from our EP3 timepoint, and both *Cdc42bpb* and *Cdc42se2* showed increased patterns of expression within the Sertoli cells taken from EP2-EP4 as compared to our control samples (Fig. 4K-N). Finally, evaluations of *Gja1* showed that in our scRNA-seq dataset, that levels of *Gja1* are highest in the control sample, before dropping dramatically where it was found to be significantly downregulated in

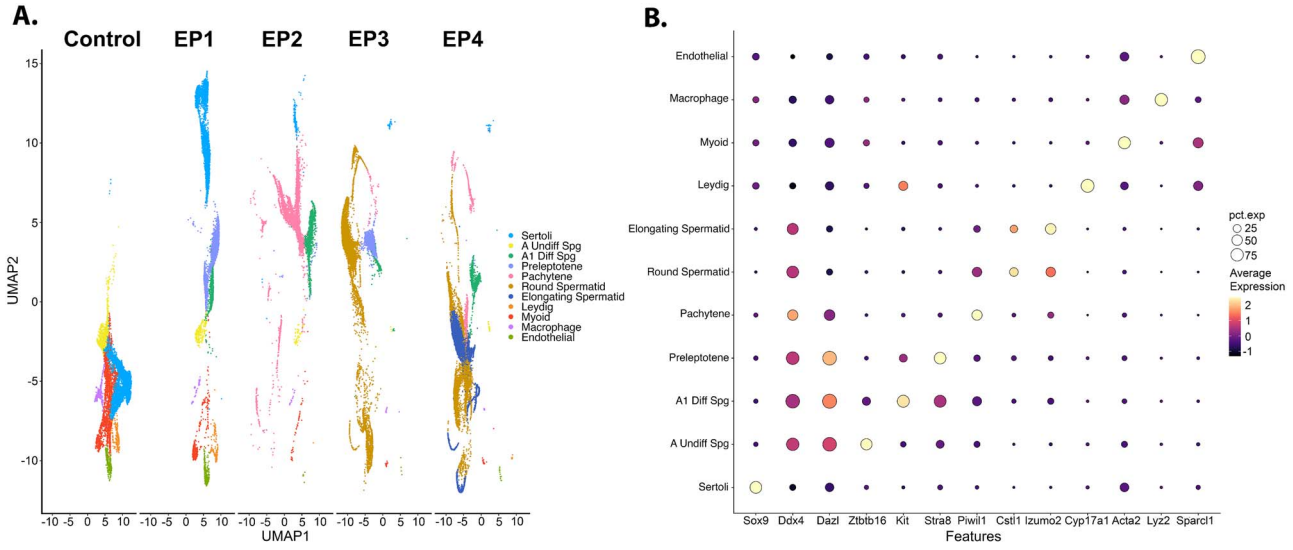

C.

	Sertoli	A Undiff Spg	A1 Diff Spg	Preleptotene	Pachytene	Round Spermatid	Elongating Spermatid	Leydig	Myoid	Macrophage	Endothelial
Control	3538	785	0	0	0	0	0	301	2199	316	317
EP1	3076	273	649	2212	0	0	0	195	501	71	395
EP2	207	50	1495	47	4346	0	0	1	46	32	5
EP3	68	3	203	1069	66	6837	0	0	45	21	4
EP4	20	32	743	8	561	3785	5534	8	40	18	13

Figure 2. (A) Uniform manifold approximation projection (UMAP) depicting the 11 identified cell types identified from the obtained single cell RNA-sequencing (scRNA-seq) dataset split between the control sample and each collected endogenous pulses 1–4 (EP1–4). Cell types include Sertoli cells, A_{undiff}, $A1_{diff}$, preleptotene spermatocytes (preleptotene), pachytene spermatocytes (pachytene), step-8 round spermatids (round spermatid), step-16 elongating spermatids (elongating spermatid), Leydig cells, myoid cells, macrophages, and endothelial cells. (B) DotPlot displaying the relative expression of marker genes for the germ and somatic cells of the testis in each assigned cell type cluster. (C) Cell numbers post-processing and quality control by timepoint and cell type. Graphs were produced using R software.

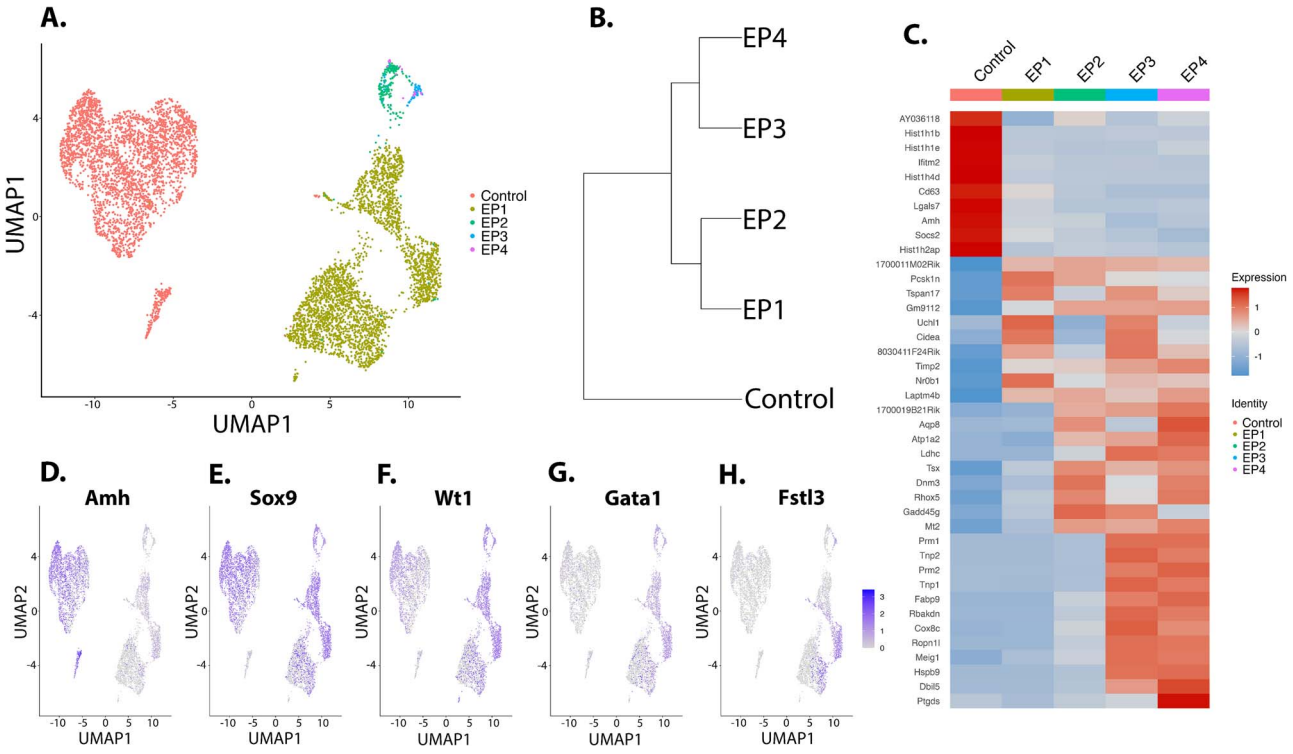

Figure 3. (A) UMAP representing all collected Sertoli cells isolated from the whole testis scRNA-seq datasets. (B) Hierarchical clustering graph depicting the primary split between the Control sample and the samples representing each collected endogenous pulse of *at*RA activity. (C) Heatmap representing the top 50 DEGs across our five collected timepoints. (D-H) DimPlots representing Sertoli cell specific expression of *Amh* (D), *Sox9* (E), *Wt1* (F), *Gata1* (G), and *Fstl3* (H). Graphs were produced using R software.

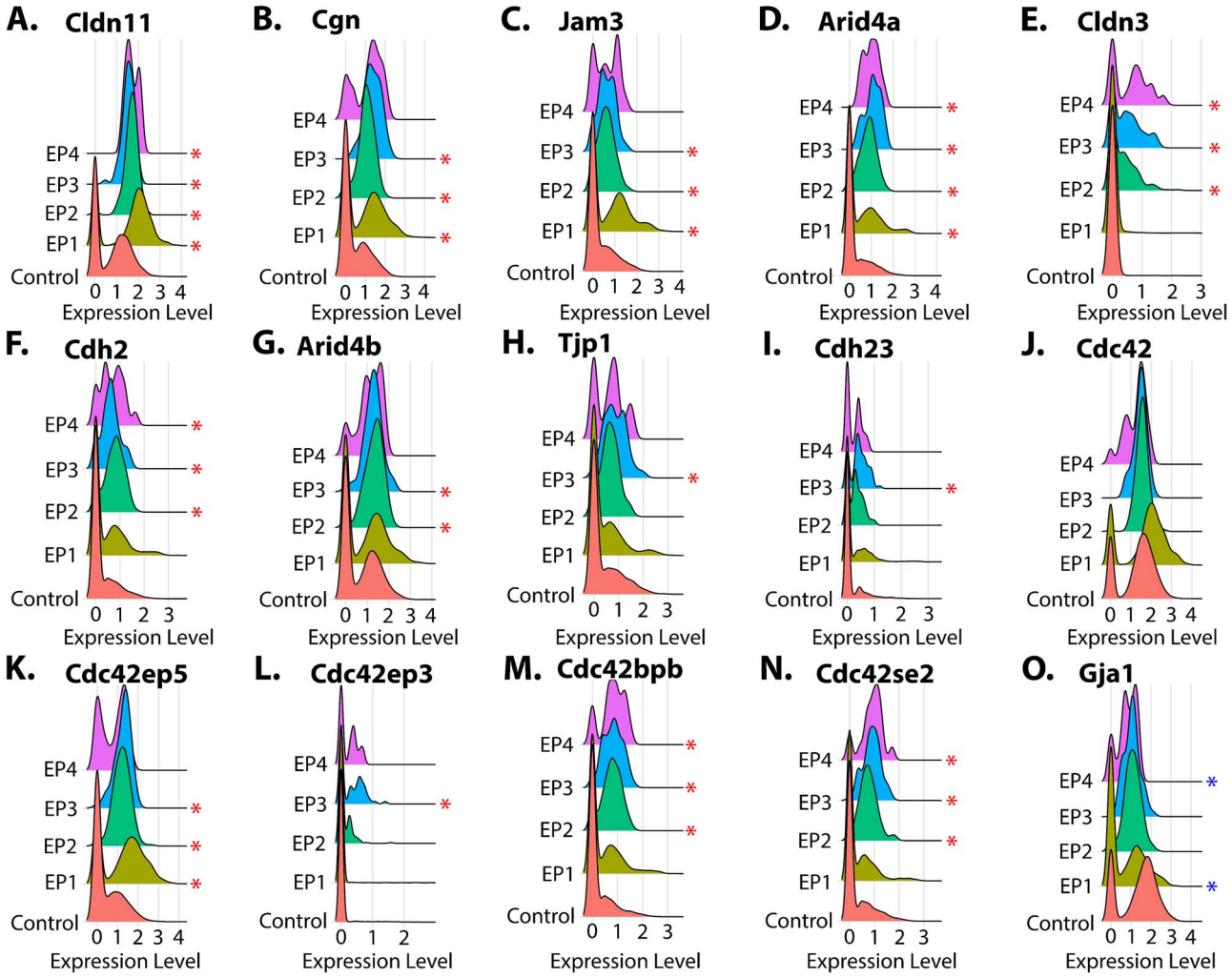

Figure 4. RidgePlots generated from the computationally isolated Sertoli cell populations depicting the expression of *Cldn11* (A), *Cgn* (B), *Jam3* (C), *Arid4a* (D), *Cldn3* (E), *Cdh2* (F), *Arid4b* (G), *Tjp1* (H), *Cdh23* (I), *Cdc42* (J), *Cdc42ep5* (K), *Cdc42ep3* (L), *Cdc42bpb* (M), *Cdc42se2* (N), and *Gja1* (O) from our scRNA-seq data. Red asterisks indicate timepoints that show significantly positive upregulation compared to the control samples, and blue asterisks represent timepoints that showed significantly negative downregulation as compared to the control samples. Graphs were produced using R software, and DEGs were calculated using log fold change ≥ 0.25 or ≤ -0.25 and adjusted *p*-value <0.05.

both the EP1 and EP4 samples (Fig. 4O). AmpliSeq analysis broadly supports these findings (see Supplemental Fig. S3 and Supplemental File S2) and together, these results described the temporal pattern of gene induction of known BTB and Sertoli-germ adhesion related genes across the first wave of spermatogenesis, where most are induced prior to meiotic initiation.

Testicular immune regulation by stage VIII–IX Sertoli cells

Evidence for an immune regulatory role by Sertoli cells has been shown repeatedly using in vitro studies [17, 45–48]. However, there is an active gap in knowledge as to when many of these actions are induced in vivo [16, 17]. In order to answer this, we identified differential gene expression of known Sertoli cell immune response genes including several serine peptidase inhibitors (*Serpina3n*, *Serpinb9*, and *Serping1* [47, 49]), CD46 antigen complement regulatory protein (*Cd46*), indoleamine 2,3-dioxygenase 1 (*Ido1* [50]), clusterin (*Clu* [51–53]), transforming growth factor beta 1 (*Tgfb1* [49]), CD55 molecule, decay accelerating factor for complement B (*Cd55b* [50, 54]), galectin 1 (*Lgals1* [55]), and C-C motif chemokine ligand 27A (*Ccl27a* [56]).

In the compiled scRNA-seq dataset, the genes *Serpina3n*, *Serpinb9*, *Serping1*, *Cd46*, and *Ido1* showed very low expression values, and were not called to be differentially expressed at any time (Fig. 5A-E). At EP1, *Clu* was highly expressed at all timepoints, including the control, but was still called as being differentially upregulated beginning at EP1 through EP4 (Fig. 5F). At EP2, *Tgfb1* was the only immune related gene found differentially upregulated, and that upregulation was maintained to the EP4 timepoint (Fig. 5G). From Sertoli cells isolated from the collected EP3 testes, *Cd55b*, *Lgals1*, and *Ccl27a* were found upregulated, and these expression patterns persisted into the captured cells at EP4, with the exception of *Lgals1* that was only upregulated at EP3, and interestingly was found to be significantly downregulated within the EP2-isolated Sertoli cells (Fig. 5H-J).

AmpliSeq results (see Supplemental Fig. S4 and Supplemental File S2) supported the findings presented from scRNA-seq analysis, and together these results showed that the induction of many regulatory immune response genes are not

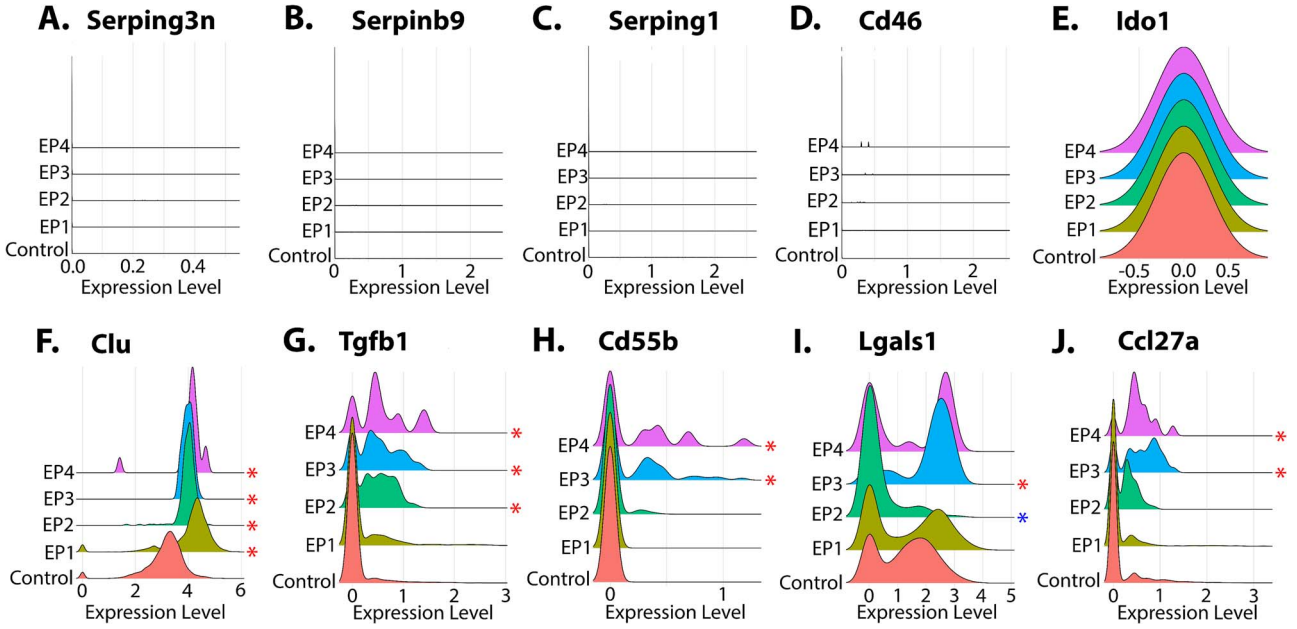

Figure 5. RidgePlots generated from the computationally isolated Sertoli cell populations depicting the expression of *Serping3n* (A), *Serpinb9* (B), *Serping1* (C), *Cd46* (D), *Ido1* (E), *Clu* (F), *Tgfb1* (G), *Cd55b* (H), *Lgals1* (I), and *Ccl27a* (J) from our scRNA-seq dataset. Red asterisks indicate timepoints that show significantly positive upregulation compared to the control samples, and blue asterisks represent timepoints that showed significantly negative downregulation as compared to the control samples. Graphs were produced using R software, and DEGs were calculated using log fold change ≥ 0.25 or ≤ -0.25 and adjusted *p*-value <0.05.

upregulated within Sertoli cells until later within spermatogenesis, possibly to support spermiogenesis and spermatid release at spermiation.

Protein secretion by stage VIII–IX Sertoli cells

Sertoli cells secrete proteins that enter the adluminal compartment to deliver nutrients to the developing germ cells [10–12, 57, 58]. Previously, the proteins that have been identified as being secreted by Sertoli cells have been grouped into five large categories: transport proteins, hormone like or growth factor like proteins, enzymes, proteins relevant to organizing the compartment of the seminiferous tubule close to the basal membrane, as well as some proteins of unknown function [16, 17]. Much of the data that has contributed to our knowledge of Sertoli cell secreted proteins was performed in vitro which cannot fully capture endogenous cell behaviors, and very little work has been done in recent years to continue to characterize these proteins [59]. As such, we identified the expression patterns of known Sertoli cell secreted genes including transferrin (Trf [60–62]), ceruloplasmin (Cp [63–65]), androgen-binding protein (*Shbg* or *Abp* when produced by Sertoli cells [66–72]), *Amh*, inhibin B (*Inhbb* [73–75]), insulin-like growth factor 1 receptor (*Igf1r* [76]), insulin-like growth factor 1 (*Igf1* [76]), plasminogen activator (*Plat* [77, 78]), and prosaposin (*Psap* [79, 80]) across the first wave of the seminiferous epithelium.

Trf was first found to be differentially upregulated within the EP3-isolated Sertoli cells, and remained differentially upregulated through the EP4 samples (Fig. 6A). *Cp* was not found to be expressed within any of our collected samples (Fig. 6B). *Shbg*, however, was, and could be seen to be differentially upregulated starting within the EP1 sample and continued to remain differentially upregulated until EP3 (Fig. 6C). *Amh* expression, when compared to the control sample, was significantly downregulated in all post-*atRA* timepoints (Fig. 6D). The genes *Inhbb*, *Igf1r*, and *Igf1* showed minimal changes in expression (Fig. 6E-G), and only *Igf1r* showed any significant change across our timepoints, being differentially upregulated only within the EP2-isolated Sertoli cells (Fig. 6F). Finally, the expression profiles of *Plat* and *Psap* showed strong increases in expression as compared to the control samples, wherein *Plat* was differentially upregulated in the EP1, EP3, and EP4 samples (Fig. 6H) and *Psap* was found to be positively differentially expressed in all post-*at*RA samples (Fig. 6I).

AmpliSeq results reiterate these findings (see Supplemental File S2 and Supplemental Fig. S5) and these data combined showed that many of the genes responsible for secreted Sertoli cell protein products were largely induced, or kept their expression high, approaching the end of the first round of spermatogenesis.

Critical *at*RA signaling genes decrease in Sertoli cells as spermatogenesis proceeds

*at*RA synthesis is known to occur during stages VIII-IX of spermatogenesis within the mouse, and much evidence has already been collected to show that Sertoli cells are responsible for producing the *at*RA responsible for initiating spermatogenesis [6, 23, 29]. However, the full mechanism has not yet been fully explained due to the shared expression of several important *at*RA pathway enzymes between testicular cell types, and the complication of asynchronous spermatogenesis. With this in mind, we sought to ask what the expression levels of genes important for *at*RA synthesis were within Sertoli cells across four successive pulses of stage VIII-IX, and whether we could further elucidate the action of Sertoli cells in synthesizing *at*RA across the cycle of the seminiferous epithelium.

Of particular emphasis to the synthesis of *at*RA are the proteins retinoid binding protein 1 (RBP1) and retinal dehydrogenase 10 (RDH10), as well as the ALDH1A family of aldehyde dehydrogenase enzymes found within the testis (ALDH1A1,

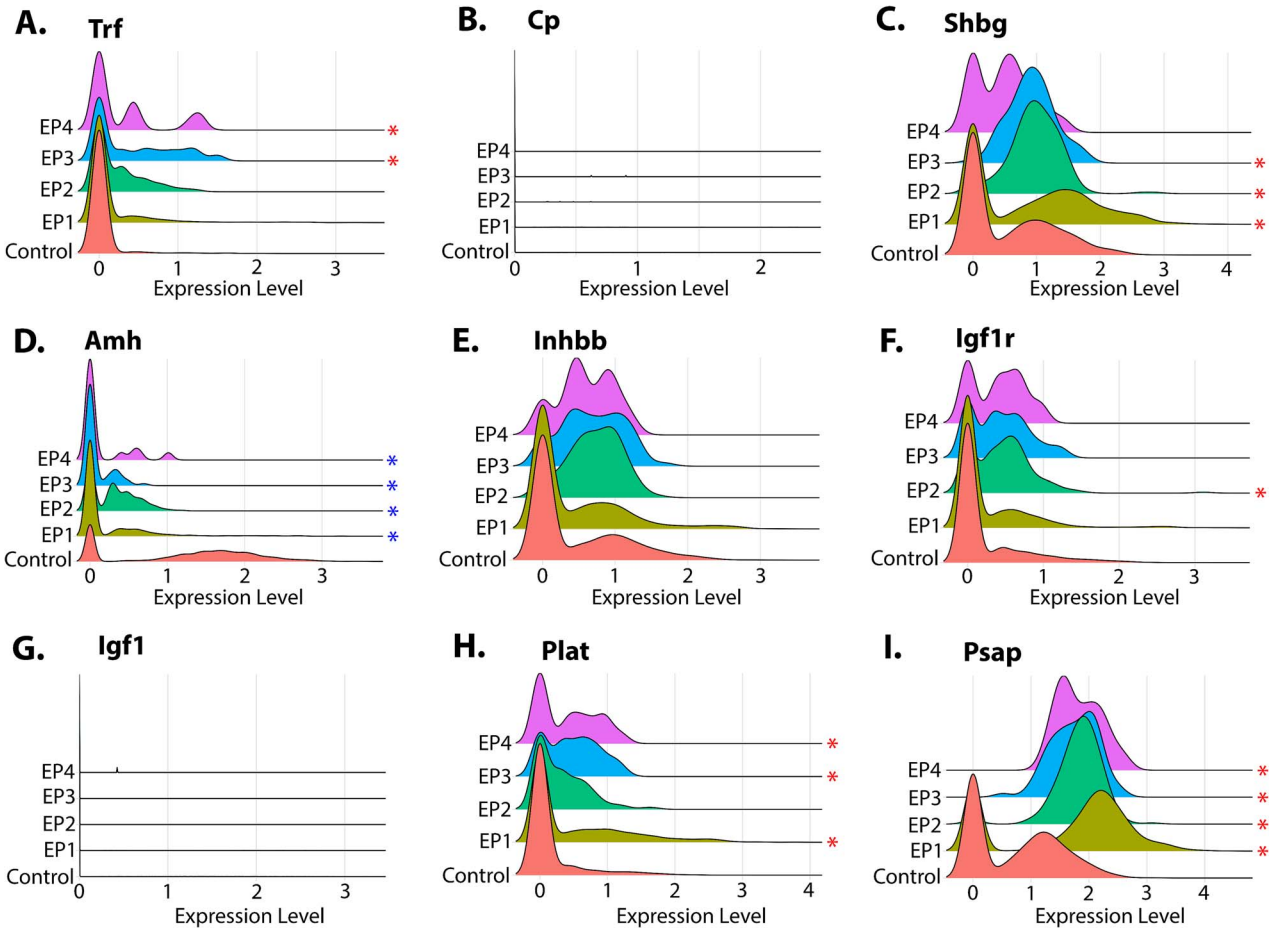

Figure 6. (A-F) RidgePlots generated from the computationally isolated Sertoli cell populations depicting the expression of *Trf* (A), *Cp* (B), *Shbg* (C), *Amh* (D), *Inhbb* (E), *Igf1r* (F), *Igf1* (G), *Plat* (H), and *Psap* (F) from our scRNA-seq data. (G/H) Red asterisks indicate timepoints that show significantly positive upregulation compared to the control samples, and blue asterisks represent timepoints that showed significantly negative downregulation as compared to the control samples. Graphs were produced using R software, and DEGs were calculated using log fold change ≥ 0.25 or ≤ -0.25 and adjusted *p*-value <0.05.

ALDH1A2, and ALDH1A3) [81–84]. RBP1 binds *all-trans* retinol (ROL), and later *all-trans* retinal (RAL), within the cell and supports the synthesis of *at*RA by protecting and shuttling retinoids to enzymes for catalysis. RDH10 is arguably the most important protein within the synthesis pathway, as it is the enzyme responsible for the rate-limiting step of the conversion of retinol to retinal. Retinal is then converted to *at*RA by the ALDH1A enzymes, mainly ALDH1A1 and ALDH1A2 that are expressed primarily in Sertoli and germ cells, respectively [19, 21].

We found from the cumulative expression data for the Sertoli and germ cells taken from our scRNA-seq experiment that Sertoli cells exhibited the highest expression of *Aldh1a1, Aldh1a2*, *Rdh10,* and *Rbp1* across all of the captured cell types (Fig. 7A). *Rdh10* levels, when evaluated by cell type across the entire timescale, appeared similar between preleptotene spermatocytes and Sertoli cells (Fig. 7A). Within both our scRNA-seq and Ampliseq data, we found that at EP1 the expression levels of *Aldh1a2*, *Rdh10*, and *Rbp1* peaked within Sertoli cells before decreasing in all subsequent time points (Fig. 7C-E). *Aldh1a1* is the exception and showed its highest expression in the pre-*at*RA Sertoli cells before decreasing in all following time points (Fig. 7B) which matched previously published work showing high *Aldh1a1* expression within the embryonic and neonatal testis [85].

These data support previous published findings that Sertoli cell synthesized *at*RA is critically important at the onset of spermatogenesis, and the decreased expression of *at*RA synthesis genes found within Sertoli cells supports the theory that as the germ cells develop they contribute to RA synthesis at stages VIII-IX.

Germ cell subtypes send specific signaling mechanisms to Sertoli cells

Previous findings have emphasized the role of germ cells in maintaining the normal functions of Sertoli cells [9, 23, 65, 86]. Sertoli cells are known to influence germ cell behavior and development, and we hypothesize that germ cells are also exerting their own influences onto their environment. This environment includes the neighboring Sertoli cells, and this effect is most likely facilitated through the extremely close associations that germ cells are required to form with Sertoli cells as they progress through the cycle of the seminiferous epithelium. To investigate this further, we employed the R package CellChat, which makes predictions by combining user supplied single cell expression data with a repository of known ligand-receptor pairs to return signaling mechanisms that are likely present between specified cell types [40].

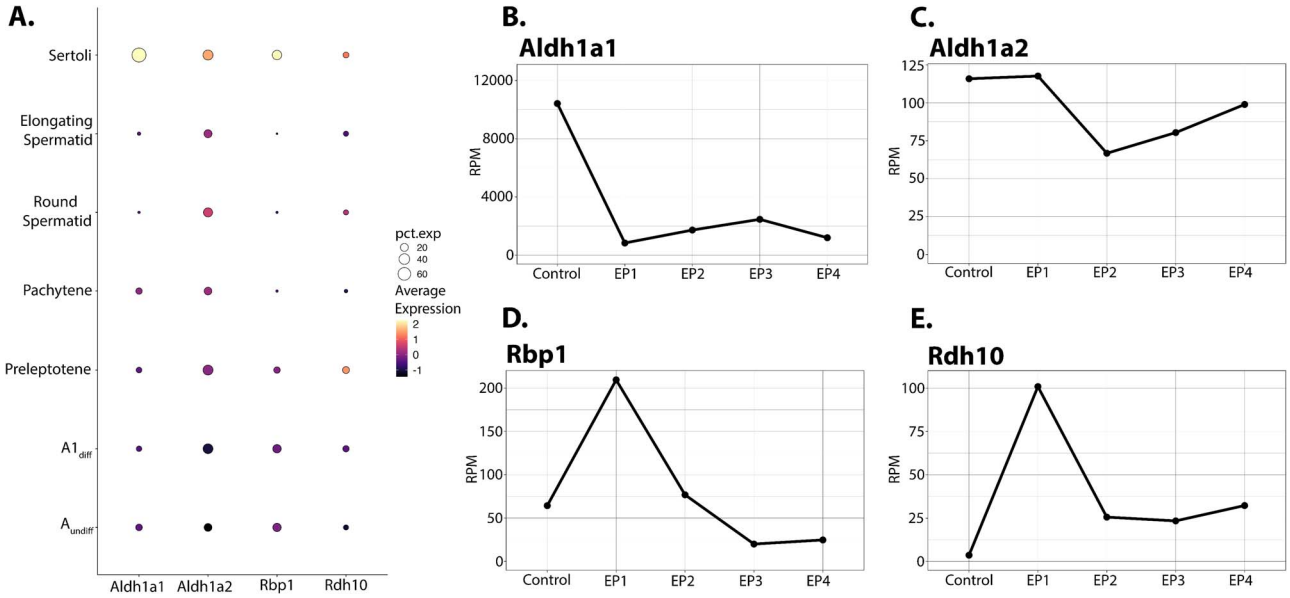

Figure 7. (A) DotPlot generated showing the aggregate mRNA expression of *Aldh1a1*, *Aldh1a2*, *Rbp1*, and *Rdh10* across the populations of A_{undiff}, $A1_{diff}$, preleptotene spermatocytes, pachytene spermatocytes, step-8 round spermatids (round spermatid), step-16 elongating spermatids (elongating spermatid), and Sertoli cells captured within our scRNA-seq datasets. (B-E) Lineplots made to represent the expression of *Aldh1a1* (B), *Aldh1a2* (C), *Rbp1* (D), and *Rdh10* (E) taken from collected AmpliSeq data compiled from FACS-isolated Sertoli cells. AmpliSeq data is presented as reads per million (RPM) and taken from pooled n = 3 AMH-Cre^{+}; RFP$^{fl/fl}$ males. Graphs were produced using R software.

All identified germ cells (A_{undiff}, $A1_{diff}$, preleptotene spermatocytes, pachytene spermatocytes, round spermatids, and elongating spermatids) were isolated from the whole testis samples, merged with the previously isolated Sertoli cells, and this resulting Seurat object underwent re-normalization and PCA analysis as described above. CellChat was then run on the resulting cells with "trim = 0.1" and "population.size = false" so the results would not be biased against the smaller populations of Sertoli cells found in the later timepoints.

These results revealed 50 signaling pathways and 727 total receptor-ligand interactions across all germ cell timepoints and populations (see Supplemental File S3). Within the control sample, prior to *at*RA treatment, 36 total receptor-ligand interactions were predicted. These numbers sharply increased following *at*RA treatment, with 171 total receptor-ligand interactions predicted at EP1, 204 at EP2, 165 at EP3, and 151 at EP4. For each timepoint unique receptor-ligand interactions were found with five, seven, seven, six, and 12 interactions predicted in each respectively (see Supplemental File S3).

There were no unique signaling pathways predicted prior to *at*RA exposure; however, there were nine that are conserved between all the post-*at*RA samples, and only predicted following *at*RA treatment: WNT, IGF, AGRN, ncWNT, CDH, GRN, THBS, SEMA5, VISFATIN. These signaling pathways alone made up 20% of all the predicted interactions within the post-*at*RA samples.

CellChat is able to identify the probable "signal sending" and "signal receiving" cells for a given interaction, and so analysis was isolated to signaling mechanisms that identified germ cell derived signals that target the Sertoli cell population within each timepoint sampled. Respectively, that included signals received by Sertoli cells from A_{undiff} in our pre-*at*RA control sample, $A1_{diff}$ and preleptotene spermatocytes at EP1, pachytene spermatocytes at EP2, round spermatids at EP3, and finally elongating spermatids at EP4. Selecting the top 10 most highly predicted signaling mechanisms at each time point, apart from the pachytene spermatocytes at EP2 and the elongating spermatids at EP4 which respectively had only had five and nine predicted, revealed information regarding how signals were sent. 55.6% of all interactions were facilitated by cell–cell contact (Fig. 8). The remaining interactions were split between ECM-receptor facilitated mechanisms (18.6%) and secreted signaling mechanisms (25.9%) (Fig. 8). Divergent behaviors were found, however, when the germ cells were evaluated individually. Cell–cell signaling made up the majority of predicted mechanisms in the A_{undiff} cells (50%), $A1_{diff}$ cells (50%), pachytene spermatocytes (60%), round spermatids (80%), and elongating spermatids (55.6%). However, secreted signaling behaviors were the majority of the predicted interactions within the preleptotene spermatocytes (50%). Secreted signaling interactions were additionally high in the $A1_{diff}$ population (40%), and the pachytene spermatocyte population (40%). ECM-receptor based signaling was highest in the A_{undiff} population (40%), but was then the lowest predicted mechanism class in all other cell types (Fig. 8).

The top 10 pathways (called by CellChat probability value) from our control samples included the signaling pathways CADM, COLLAGEN, NOTCH, JAM, LAMININ, FN1, and PSAP. At EP1 there were two new cell types present: the $A1_{diff}$ and preleptotene spermatocytes. Both cell types contained CADM, MK, FN1, JAM, and PSAP within the top 10 highest predicted signaling mechanisms called, and all signaling pathways shared the same predicted receptor-ligand signaling pairs. Unique to the $A1_{diff}$ cells is the MPZ pathway and unique to the preleptotene spermatocytes at this timepoint is the MIF pathway. The pachytene spermatocytes that were captured at EP2 only returned five predicted signaling pathways: MIF, NOTCH, PSAP, and MPZ. EP3 introduced the first generation of produced spermatids, and predicted signaling mechanisms at this time included THBS, NOTCH, CD39, CDH, COLLAGEN, JAM, and CD96. Finally, when we analyzed the predicted signals that originated from

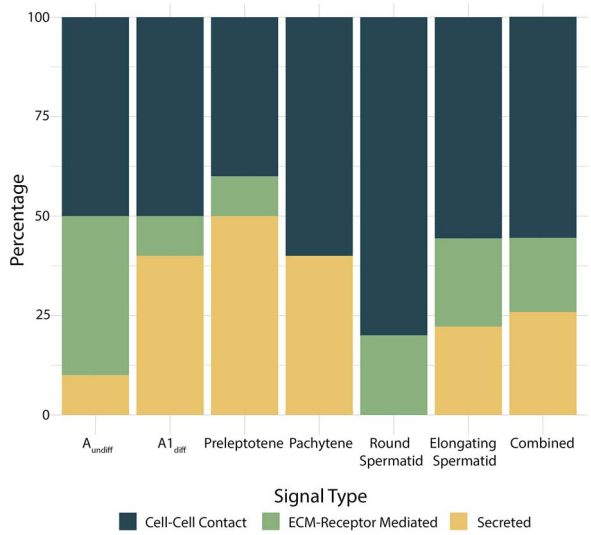

Figure 8. Stack plot representing the proportional distribution of predicted signaling types presented by germ cell subtypes. Columns represent A undifferentiated spermatogonia (A_{undiff}), A1 differentiating spermatogonia ($A1_{diff}$), preleptotene spermatocytes, pachytene spermatocytes, step-8 round spermatids (round spermatid), step-16 elongating spermatids (elongating spermatid), and finally as an average of all germ cell types (Combined). The included graph was produced using R software.

step-16 elongated spermatids at EP4, only nine mechanisms were predicted and they included THBS, NOTCH, COLLAGEN, CD39, ADIPONECTIN, and CD96.

All of the above data suggested that (i) differentiating germ cells that have been exposed to *at*RA are more active in communicating to Sertoli cells, (ii) germ cells primarily used cell–cell contact mediated signaling mechanisms, and (iii) each germ cell subtype that could be identified within our data had a unique pattern of signaling behaviors used to influence nearby Sertoli cells.

Discussion

Previously published results have characterized the Sertoli cell transcriptome in adult, synchronized animals and identified peak expression patterns of many genes coinciding with stage progression through spermatogenesis [23]. Here, we have expanded on these results by focusing on one point within the cycle of the seminiferous epithelium, stages VIII–IX, which coincides with *at*RA synthesis and several major testicular differentiation and remodeling events. We tracked the expression of known functional Sertoli cell genes throughout four successive occurrences of these stages. This time scale allowed us to track Sertoli cell behaviors starting prior to the onset of spermatogenesis, throughout one complete round of spermatogenesis, and culminating in the release of the first generation of elongated spermatids during spermiation. The data analyzed and described within this work demonstrated our successful capture of the pre- and post-pubertal state of the testis, which has allowed us to accurately determine when known Sertoli cell expressed genes are induced in each of the post-*at*RA samples, and which genes showed expression prior to the initiation of spermatogenesis coinciding with *at*RA exposure. We additionally sought to investigate germ-Sertoli cell signaling behaviors, and used computational analysis to predict receptor-ligand binding pairs present on germ and Sertoli cells at each timepoint [23, 40].

Previous studies have shown the difficulty in separating testicular cell-types for analysis, especially Sertoli and germ cells due to the adherent junctions formed between them to support the germ cells through the seminiferous epithelium as they develop [22, 23, 34]. In this study, we have utilized scRNA-seq technology to provide single cell resolution of whole testes taken periodically across one complete round of spermatogenesis. Marker gene analysis supported that we have isolated cell types with high specificity (Fig. 2B); however, only certain populations could be successfully isolated in a large quantity. Interstitial cell types including myoid cells, macrophages, and Leydig cells could only be captured in small numbers, and this is likely the result of how tissue was handled prior to library preparation. Our dissociation protocol allowed for high capture of the germ and Sertoli cells contained within the seminiferous tubules; however, the repetitious wash steps that the tubules were exposed to following detunication likely depleted the available pools of interstitial cells. Further studies interested in analysis of interstitial cell populations or of adult isolated Sertoli cells will likely need to take a different approach to their library construction, either by an alternative dissociation method that is gentler on the interstitial cells or by enriching their selected populations for the desired cell types.

Additionally, our captured Sertoli cell populations shrunk dramatically with increasing age. As germ cells divide, and fill the tubule interior, Sertoli cells eventually make up only ~3% of the total cells contained within the seminiferous tubules [87]. To validate our scRNA-seq results we additionally performed AmpliSeq on mechanically sorted Sertoli cells, which followed the scRNA-seq data closely. Some diverging results were found between the two datasets however, as in the case of *Cgn, Jam3, Cldn3, Cdh2, Tjp1,* and *Cdh23*. We believe that differences found between the two methods are likely due to the non-normality of scRNA-seq data inherent due to technical noise and dropouts [88], or potentially contaminating cell types present within the AmpliSeq results. Although mechanical sorting is very efficient, we cannot completely eliminate any chance of germ cells or other testicular somatic cells following the collected Sertoli cells during FACS. Additionally, our AmpliSeq dataset is not as robust as the results obtained from scRNA-seq as only 23 930 genes from the *Mus musculus* genome are included within AmpliSeq sequencing, and while the vast majority of our genes of interest could be compared, we were not able to measure the expression of *Trf* or *Gja1* using AmpliSeq analysis.

Through this work, we have evaluated the expression patterns of many genes that are known to be expressed by Sertoli cells and regulate many of this cell population's functions. Several important tight junction forming genes that are known to be essential to the formation of the BTB barrier are induced during the first endogenous pulse of *at*RA activity including *Cldn11*, *Cgn*, *Jam3*, and *Ardi4a* that could suggest these transcripts are critical to the initial establishment of the BTB, and the first movement of germ cells across the BTB into the adluminal compartment. Transgenic studies evaluating *Arid4a* knockout animals in particular have shown the essential role of *Arid4a* in sustaining meiotic progression and the maintenance of the BTB [51]. Later timepoints revealed additional upregulated BTB/cell-adhesion related transcripts, and several downstream effectors of CDC42 activity including *Cdc42ep3, Cdc42ep5, Cdc42bpb,* and *Cdc42se2*. The late

induction of these genes supports their roles in the development and formation of tight cellular associations between spermatocytes and spermatids with neighboring Sertoli cells formed during later rounds of germ cell differentiation. This idea is supported by previously published findings regarding CDC42 activity, as in vivo work using a *Cdc42* knockout model showed that *Cdc42* is not critical to the onset of spermatogenesis, but rather is needed for the steady-state production of sperm [42]. Our data corroborated this and showed peak expression of many *Cdc42* effector genes just prior to, and during spermiogenesis.

Immune regulation is an essential function of Sertoli cells, and this function is carried out in several ways: the maintenance of the BTB acts as a physical, semi-permeable barrier to prevent immune cells from entering the testis, complement inhibition, immunoregulatory environmental control, and phagocytosis of dead and dying cells, among others [46, 48, 54, 89]. Previous studies showed that Sertoli cells are able to provide immune protection to co-grafted cells of non-testicular origin and have a unique ability to survive following transplantation across xenografts and allografts [50]. It is also known that Sertoli cells are not only able to suppress an immune response, but also capable of inducing regulatory immune cells (macrophages and T cells) to maintain the testicular microenvironment [45, 46, 48, 54, 56, 90, 91]. At EP1, *Clu* is the only immune response gene found to be differentially upregulated, and its expression remained high throughout our entire dataset. Clusterin has been observed to be ubiquitously expressed by secretory cells, and is a known complement inhibitor produced by Sertoli cells with a known role in inhibiting the complement response and preventing compliment response mediated cytolysis [53, 92, 93]. We predict that the consistently high expression of *Clu* is likely the result of innate, immunoprotective actions of Sertoli cells, initiate at the start of spermatogenesis to protect the germ cell populations. Other immune related transcripts are found differentially upregulated in Sertoli cells isolated from our later EP2 and EP3 timepoints, which stayed consistently high until EP4, and included other complement inhibitors, immunomodulatory factors, and chemokines. The delayed expression of these components may suggest that the immune regulatory functions of Sertoli cells are most important to support the spermatocytes and spermatids through their final rounds of meiotic progression and maturation; however, further validation will be needed to support this claim.

Tracking known Sertoli cell expressed genes that encode functional secreted protein products followed a similar pattern to the immune related genes; many of the genes evaluated were not differentially upregulated until round spermatids were formed first at EP3 with this expression pattern being carried to EP4 suggesting that many of the genes important for Sertoli cell secreted products are most integral during spermiogenesis and spermiation. As the Sertoli cells continue developing and are exposed to various differentiating populations of germ cells, they are likely being stimulated by their environment to carry out a continually increasing workload of tasks within the seminiferous tubules of the testis including the reconstruction of the BTB following germ cell migration between tubule compartments, regulating hormone synthesis, and supporting spermatid compaction. Many of the known functions of the Sertoli cell secreted proteins have been found using in vitro studies, however, and will require further in vivo validation to make their roles in the testis clear.

*at*RA production is critical, and the initiation of spermatogenesis depends on it. Without Sertoli cell synthesized *at*RA, spermatozoa will never be formed and the individual will be infertile [19, 21]. Previous work showed that critical genes required for synthesizing *at*RA within Sertoli cells peaked in their expression levels during stages VII–VIII in the adult mouse testis. Published genetic studies showed that Sertoli cells deficient in the critical *at*RA synthesis enzyme coding genes (*Aldh1a1/1a2/1a3*) were unable to clear the A to A1 transition, but treatment with exogenous *at*RA allowed for spermatogenesis to reinitiate and continue [19]. Subsequent studies performed on mice with cell specific ablation of *Aldh1a1/1a2* corroborated these findings, and together provide strong evidence that Sertoli cell derived *at*RA is essential for the initiation of spermatogenesis [20]. Interestingly, other studies have shown that germ cells are able to produce additional *at*RA, suggesting that they may act to supplement Sertoli cell derived *at*RA in the adult testis [19, 21, 23, 94]. Our data showed that Sertoli cells express *at*RA synthesis specific enzyme coding genes within all of our sequenced time points, however the expression levels of *Rdh10*, *Aldh1a1*, *Aldh1a2*, and *Rbp1* all dropped significantly with time after the first endogenous pulse (Fig. 7A-E). Meanwhile, levels of *Rdh10* were comparable between preleptotene spermatocytes and Sertoli cells, and *Aldh1a2* expression was found to be moderately expressed in all germ cell subtypes (Fig. 7A). Further evaluations will be needed; however, the transcriptional data presented here support previous studies, which asserted that Sertoli cell synthesized *at*RA is essential for the first endogenous pulse of *at*RA needed to clear the A to A1 transition, and that germ cells may also support continual spermatogenesis by producing RAL or *at*RA.

Finally, our evaluations of cell–cell signaling as predicted by the R package CellChat yielded multiple interesting results. Cell–cell signaling was found to be the most abundant method by which germ and Sertoli cells may be communicating, and this corroborated our hypothesis, that germ-Sertoli cell signaling mechanisms were likely facilitated by the close spatial associations these cells form throughout spermatogenesis. Prior to the start of spermatogenesis, A_{undiff} cells were predicted to be most likely communicating to Sertoli cells using the following pathways: CADM, COLLAGEN, NOTCH, JAM, LAMININ, FN1, and PSAP, which have been implicated in a variety of cellular functions including extracellular matrix remodeling, cell–cell adhesion, stem cell population maintenance, and the establishment of basement membranes supporting that these signaling pathways likely represent germ cell influence to establish the germinal epithelium prior to the initiation of spermatogenesis [95–99]. Later timepoints produced additional signaling pathways, including MK, MIF, MPZ, THBS, CD39, CDH, CD96, and ADIPONECTIN. These pathways have known roles spanning cell differentiation and survival, cell migration, immune response regulation, cell adhesion, tissue remodeling, and BTB maintenance supporting germ cells through their meiotic divisions and maturation following the *at*RA response [100–107]. Interestingly, the $A1_{diff}$ and preleptotene spermatocytes showed many similarities in signaling mechanism and ligand-receptor pairs predicted, which displayed that these cell types are likely very similar in the effects they exert on their neighboring Sertoli cells. Overall, the divergent functions of the predicted pathways identified from the post-*at*RA samples compared to the pathways predicted prior to *at*RA exposure

represent what is likely a pattern of induced behavior following the initiation of spermatogenesis. Further work targeting Sertoli- or germ-specific ligands/signaling receptors predicted by next generation technology may provide valuable insights into currently unknown pathways that are essential to spermatozoa production and the successful continuation of spermatogenesis.

In conclusion, this work provides a comprehensive study of Sertoli cell transcriptional change during stages VIII–IX spanning across the first round of spermatogenesis and characterizes germ-Sertoli cell signaling mechanisms that may be occurring between each germ cell subtype formed during stages VIII-IX and the Sertoli cells that flank them. Furthering our understanding of the dynamic behaviors of Sertoli cells across the cycle of the seminiferous epithelium, and how they serve to support germ cell development and growth, will be central to future medical innovation made in the field of male reproductive biology. It is our hope that this work, and the high-resolution data produced regarding Sertoli cell gene expression, will be of use to the development of future treatments and diagnostic tools to resolve cases of idiopathic male infertility.

Acknowledgment

The authors thank Lisette Maddison, Deqiang Miao, and Mark Wildung at the Washington State University Laboratory for Biotechnology and Bioanalysis for sequencing library preparation as well as initial AmpliSeq data processing, Melissa Oatley and the Center for Reproductive Biology FACS Core for their assistance with sorting and obtaining cells for AmpliSeq analysis, as well as Traci Topping and Crystal Lawson for technical assistance and helpful discussion.

Supplementary Data

Supplementary data are available at *BIOLRE* online.

Conflict of interest: The authors declare no conflicts of interest.

Author Contributions

Project conceptualization (MG and SH), Data acquisition (SH), Manuscript writing and editing (SH and MG), Analysis (SH and MG), Figures (SH), Funding acquisition (MG).

Data availability

Raw and processed data referenced within this work have been made available through NCBI's Gene Expression Omnibus (GEO) database and can be accessed with the GEO series accession number GSE259354. Additional interactive visualization of the contained scRNA-seq data can be found at https://cvm106v.vetmed.wsu.edu/datahub/Griswold/.

References

1. How common is infertility? | NICHD – Eunice Kennedy Shriver National Institute of Child Health and Human Development; 2018. https://www.nichd.nih.gov/health/topics/infertility/conditioninfo/common. Accessed 6 August 2022.
2. Agarwal A, Mulgund A, Hamada A, Chyatte MR. A unique view on male infertility around the globe. *Reprod Biol Endocrinol* 2015; **13**:37.
3. Kothandaraman N, Agarwal A, Abu-Elmagd M, Al-Qahtani MH. Pathogenic landscape of idiopathic male infertility: new insight towards its regulatory networks. *NPJ Genom Med* 2016; **1**:16023.
4. Russell LD, Ettlin RA, Hikim APS, Clegg ED. Histological and histopathological evaluation of the testis. *Int J Androl* 1993; **16**: 83–83.
5. Stem cells in the testis. *Int J Exp Pathol* 1998; **79**:67–80.
6. Griswold MD. Spermatogenesis: the commitment to meiosis. *Physiol Rev* 2016; **96**:1–17.
7. Evans E, Hogarth C, Mitchell D, Griswold M. Riding the Spermatogenic wave: profiling gene expression within neonatal germ and Sertoli cells during a synchronized initial wave of spermatogenesis in Mice1. *Biol Reprod* 2014; **90**:1–12.
8. Yoshida S, Sukeno M, Nakagawa T, Ohbo K, Nagamatsu G, Suda T, Nabeshima Y. The first round of mouse spermatogenesis is a distinctive program that lacks the self-renewing spermatogonia stage. *Development* 2006; **133**:1495–1505.
9. Mruk DD, Cheng CY. Sertoli-Sertoli and Sertoli-germ cell interactions and their significance in germ cell movement in the seminiferous epithelium during spermatogenesis. *Endocr Rev* 2004; **25**: 747–806.
10. Griswold MD. 50 years of spermatogenesis: Sertoli cells and their interactions with germ cells. *Biol Reprod* 2018; **99**:87–100.
11. Griswold MD. The central role of Sertoli cells in spermatogenesis. *Semin Cell Dev Biol* 1998; **9**:411–416.
12. França LR, Hess RA, Dufour JM, Hofmann MC, Griswold MD. The Sertoli cell: one hundred fifty years of beauty and plasticity. *Andrology* 2016; **4**:189–212.
13. Cheng CY, Mruk DD. The blood-testis barrier and its implications for male contraception. *Pharmacol Rev* 2012; **64**:16–64.
14. Mruk DD, Cheng CY. The mammalian blood-testis barrier: its biology and regulation. *Endocr Rev* 2015; **36**:564–591.
15. Oatley MJ, Racicot KE, Oatley JM. Sertoli cells dictate Spermatogonial stem cell niches in the mouse Testis1. *Biol Reprod* 2011; **84**:639–645.
16. Griswold MD, McLean D. Sertoli cell function and protein secretion. In: Skinner MK, Griswold MD (eds.), *Sertoli Cell Biology*. Cambridge: Academic Press; 2005: 95–106.
17. Griswold MD. Protein secretions of Sertoli cells. *Int Rev Cytol* 1988; **110**:133–156.
18. Gewiss R, Topping T, Griswold MD. Cycles, waves, and pulses: retinoic acid and the organization of spermatogenesis. *Andrology* 2020; **8**:892–897.
19. Teletin M, Vernet N, Yu J, Klopfenstein M, Jones JW, Féret B, Kane MA, Ghyselinck NB, Mark M. Two functionally redundant sources of retinoic acid secure spermatogonia differentiation in the seminiferous epithelium. *Development* 2019; **146**:dev170225.
20. Agrimson KS, Onken J, Mitchell D, Topping TB, Chiarini-Garcia H, Hogarth CA, Griswold MD. Characterizing the Spermatogonial response to retinoic acid during the onset of spermatogenesis and following synchronization in the neonatal mouse testis. *Biol Reprod* 2016; **95**:81.
21. Topping T, Griswold MD. Global deletion of ALDH1A1 and ALDH1A2 genes does not affect viability but blocks spermatogenesis. *Front Endocrinol* 2022; **13**:871225.
22. Green CD, Ma Q, Manske GL, Shami AN, Zheng X, Marini S, Moritiz L, Sultan C, Gurczynski SJ, Moore BB, Tallquist MD, Li JZ, *et al.* A comprehensive roadmap of murine spermatogenesis defined by single-cell RNA-seq. *Dev Cell* 2018; **46**:651–667.e10.
23. Gewiss RL, Law NC, Helsel AR, Shelden EA, Griswold MD. Two distinct Sertoli cell states are regulated via germ cell crosstalk†. *Biol Reprod* 2021; **105**:1591–1602.
24. Schleif MC, Havel SL, Griswold MD. Function of retinoic acid in development of male and female gametes. *Nutrients* 2022; **14**:1293.
25. Hogarth CA, Evanoff R, Snyder E, Kent T, Mitchell D, Small C, Amory JK, Griswold MD. Suppression of Stra8 expression in the mouse gonad by WIN 18,4461. *Biol Reprod* 2011; **84**:957–965.
26. Hogarth CA, Evanoff R, Mitchell D, Kent T, Small C, Amory JK, Griswold MD. Turning a Spermatogenic wave into a tsunami:

synchronizing murine spermatogenesis using WIN 18,4461. *Biol Reprod* 2013; **88**:1–9.
27. Paik J, Haenisch M, Muller CH, Goldstein AS, Arnold S, Isoherranen N, Brabb T, Treuting PM, Amory JK. Inhibition of retinoic acid biosynthesis by the Bisdichloroacetyldiamine WIN 18,446 markedly suppresses spermatogenesis and alters retinoid metabolism in mice. *J Biol Chem* 2014; **289**: 15104–15117.
28. Lécureuil C, Fontaine I, Crepieux P, Guillou F. Sertoli and granulosa cell-specific Cre recombinase activity in transgenic mice. *Genesis* 2002; **33**:114–118.
29. Hess RA, de Franca LR. Spermatogenesis and Cycle of the Seminiferous Epithelium. In: Cheng CY (ed.), *Molecular Mechanisms in Spermatogenesis*. New York, NY: Springer; 2008: 1–15.
30. Meistrich ML, Hess RA. Assessment of Spermatogenesis Through Staging of Seminiferous Tubules. In: Carrell DT, Aston KI (eds.), *Spermatogenesis: Methods and Protocols*. Totowa, NJ: Humana Press; 2013: 299–307.
31. Zheng GXY, Terry JM, Belgrader P, Ryvkin P, Bent ZW, Wilson R, Ziraldo SB, Wheeler TD, McDermott GP, Zhu J, Gregory MT, Shuga J, *et al.* Massively parallel digital transcriptional profiling of single cells. *Nat Commun* 2017; **8**:14049.
32. Hao Y, Hao S, Andersen-Nissen E, Mauck WM, Zheng S, Butler A, Lee MJ, Wilk AJ, Darby C, Zager M, Hoffman P, Stoeckius M, *et al.* Integrated analysis of multimodal single-cell data. *Cell* 2021; **184**:3573–3587.e29.
33. McGinnis CS, Murrow LM, Gartner ZJ. Doublet finder: doublet detection in single-cell RNA sequencing data using artificial nearest Neighbors. *Cell Systems* 2019; **8**:329–337.e4.
34. Hermann BP, Cheng K, Singh A, Roa-De La Cruz L, Mutoji KN, Chen I-C, Gildersleeve H, Lehle JD, Mayo M, Westernströer B, Law NC, Oatley MJ, *et al.* The mammalian spermatogenesis single-cell transcriptome, from Spermatogonial stem cells to spermatids. *Cell Rep* 2018; **25**:1650–1667.e8.
35. Jeanes A, Wilhelm D, Wilson MJ, Bowles J, McClive PJ, Sinclair AH, Koopman P. Evaluation of candidate markers for the peritubular myoid cell lineage in the developing mouse testis. *Reproduction* 2005; **130**:509–516.
36. Ademi H, Djari C, Mayère C, Neirijnck Y, Sararols P, Rands CM, Stévant I, Conne B, Nef S. Deciphering the origins and fates of steroidogenic lineages in the mouse testis. *Cell Rep* 2022; **39**:110935.
37. Klingler A, Regensburger D, Tenkerian C, Britzen-Laurent N, Hartmann A, Stürzl M, Naschberger E. Species-, organ- and cell-type-dependent expression of SPARCL1 in human and mouse tissues. *PloS One* 2020; **15**:e0233422.
38. Chen Y, Zheng Y, Gao Y, Lin Z, Yang S, Wang T, Wang Q, Xie N, Hua R, Liu M, Sha J, Griswold MD, *et al.* Single-cell RNA-seq uncovers dynamic processes and critical regulators in mouse spermatogenesis. *Cell Res* 2018; **28**:879–896.
39. Maclean JA, Chen MA, Wayne CM, Bruce SR, Rao M, Meistrich ML, Macleod C, Wilkinson MF. Rhox: a new homeobox gene cluster. *Cell* 2005; **120**:369–382.
40. Jin S, Guerrero-Juarez CF, Zhang L, Chang I, Ramos R, Kuan C-H, Myung P, Plikus MV, Nie Q. Inference and analysis of cell-cell communication using cell chat. *Nat Commun* 2021; **12**:1088.
41. Li W, Turner A, Aggarwal P, Matter A, Storvick E, Arnett DK, Broeckel U. Comprehensive evaluation of Ampli Seq transcriptome, a novel targeted whole transcriptome RNA sequencing methodology for global gene expression analysis. *BMC Genomics* 2015; **16**:1069.
42. Heinrich A, Bhandary B, Potter SJ, Ratner N, DeFalco T. Cdc42 activity in Sertoli cells is essential for maintenance of spermatogenesis. *Cell Rep* 2021; **37**:109885.
43. Erickson JW, Cerione RA. Multiple roles for Cdc42 in cell regulation. *Curr Opin Cell Biol* 2001; **13**:153–157.
44. Sridharan S, Brehm R, Bergmann M, Cooke PS. Role of Connexin 43 in Sertoli cells of testis. *Ann N Y Acad Sci* 2007; **1120**: 131–143.
45. Kaur G, Mital P, Dufour JM. Testisimmune privilege - assumptions versus facts. *Anim Reprod* 2013; **10**:3–15.
46. Meinhardt A, Hedger MP. Immunological, paracrine and endocrine aspects of testicular immune privilege. *Mol Cell Endocrinol* 2011; **335**:60–68.
47. Sipione S, Simmen KC, Lord SJ, Motyka B, Ewen C, Shostak I, Rayat GR, Dufour JM, Korbutt GS, Rajotte RV, Bleackley RC. Identification of a novel human Granzyme B inhibitor secreted by cultured Sertoli Cells1. *The Journal of Immunology* 2006; **177**: 5051–5058.
48. Doyle TJ, Kaur G, Putrevu SM, Dyson EL, Dyson M, McCunniff WT, Pasham MR, Kim KH, Dufour JM. Immunoprotective properties of primary Sertoli cells in mice: potential functional pathways that confer immune Privilege1. *Biol Reprod* 2012; **86**: 1–14.
49. Lui W-Y, Lee WM, Cheng CY. TGF-βs: their role in testicular function and Sertoli cell tight junction dynamics. *Int J Androl* 2003; **26**:147–160.
50. Washburn RL, Martinez-Marin D, Korać K, Sniegowski T, Rodriguez AR, Chilton BS, Hibler T, Pruitt K, Bhutia YD, Dufour JM. The Sertoli cell complement signature: a suspected mechanism in xenograft survival. *Int J Mol Sci* 2023; **24**:1890.
51. Bailey R, Griswold MD. Clusterin in the male reproductive system: localization and possible function. *Mol Cell Endocrinol* 1999; **151**:17–23.
52. Clark AM, Griswold MD. Expression of clusterin/sulfated glycoprotein-2 under conditions of heat stress in rat Sertoli cells and a mouse Sertoli cell line. *J Androl* 1997; **18**:257–263.
53. Tschopp J, Chonn A, Hertig S, French LE. Clusterin, the human apolipoprotein and complement inhibitor, binds to complement C7, C8 beta, and the b domain of C9. *J Immunol* 1993; **151**: 2159–2165.
54. Washburn RL, Dufour JM. Complementing testicular immune regulation: the relationship between Sertoli cells, complement, and the immune response. *Int J Mol Sci* 2023; **24**:3371.
55. Lei T, Moos S, Klug J, Aslani F, Bhushan S, Wahle E, Fröhlich S, Meinhardt A, Fijak M. Galectin-1 enhances TNFα-induced inflammatory responses in Sertoli cells through activation of MAPK signalling. *Sci Rep* 2018; **8**:3741.
56. Guazzone VA, Jacobo P, Theas MS, Lustig L. Cytokines and chemokines in testicular inflammation: a brief review. *Microsc Res Tech* 2009; **72**:620–628.
57. Petersen C, Söder O. The Sertoli cell – a hormonal target and 'super' nurse for germ cells that determines testicular size. *Horm Res* 2006; **66**:153–161.
58. O'Donnell L, Smith LB, Rebourcet D. Sertoli cells as key drivers of testis function. *Semin Cell Dev Biol* 2022; **121**:2–9.
59. Saewu A, Kongmanas K, Raghupathy R, Netherton J, Kadunganattil S, Linton J-J, Chaisuriyong W, Faull KF, Baker MA, Tanphaichitr N. Primary Sertoli cell cultures from adult mice have different properties compared with those derived from 20-day-old animals. *Endocrinology* 2019; **161**:bqz020.
60. Sylvester SR, Griswold MD. The testicular iron shuttle: a 'nurse' function of the Sertoli cells. *J Androl* 1994; **15**:381–385.
61. Skinner MK, Griswold MD. Sertoli cells synthesize and secrete transferrin-like protein. *J Biol Chem* 1980; **255**:9523–9525.
62. Lee NT, Chae CB, Kierszenbaum AL. Contrasting levels of transferrin gene activity in cultured rat Sertoli cells and intact seminiferous tubules. *Proc Natl Acad Sci* 1986; **83**:8177–8181.
63. Mather JP. Ceruloplasmin, a copper-transport protein, can act as a growth promoter for some cell lines in serum-free medium. *In Vitro* 1982; **18**:990–996.
64. Skinner MK, Griswold MD. Sertoli cells synthesize and secrete a ceruloplasmin-like protein. *Biol Reprod* 1983; **28**:1225–1229.
65. Onoda M, Djakiew D. Pachytene spermatocyte protein(S) stimulate Sertoli cells grown in bicameral chambers: dose-dependent secretion of Ceruloplasmin, Sulfated Glycoprotein-1, Sulfated Glycoprotein-2, and transferrin. *In Vitro Cell Dev Biol* 1991; **27A**:215–222.

66. Tindall DJ, Schrader WT, Means AR. The Production of Androgen Binding Protein by Sertoli Cells. In: Dufau ML, Means AR (eds.), *Hormone Binding and Target Cell Activation in the Testis*. Boston, MA: Springer US; 1974: 167–175.
67. Steinberger A, Walther J, Heindel JJ, Sanborn BM, Tsai Y-H, Steinberger E. Hormone interactions in the Sertoli cells. *In Vitro* 1979; **15**:23–31.
68. Courot M. ABP: the testicular protein that binds androgens. *Reprod Nutr Dev* 1980; **20**:587–591.
69. Hansson V, Weddington SC, French FS, McLean W, Smith A, Nayfeh SN, Ritzén EM, Hagenäs L. Secretion and role of androgen-binding proteins in the testis and epididymis. *J Reprod Fertil Suppl* 1976; **24**:17–33.
70. Kierszenbaum AL, Feldman M, Lea O, Spruill WA, Tres LL, Petrusz P, French FS. Localization of androgen-binding protein in proliferating Sertoli cells in culture. *Proc Natl Acad Sci* 1980; **77**:5322–5326.
71. O'Shaughnessy PJ, Monteiro A, Verhoeven G, De Gendt K, Abel MH. Effect of FSH on testicular morphology and spermatogenesis in gonadotrophin-deficient hypogonadal mice lacking androgen receptors. *Reproduction* 2010; **139**:177–184.
72. Joseph DR, Sullivan PM, Wang YM, Millhorn DE, Bayliss DM. Complex structure and regulation of the ABP/SHBG gene. *J Steroid Biochem Mol Biol* 1991; **40**:771–775.
73. Rodriguez KF, Brown PR, Amato CM, Nicol B, Liu C-F, Xu X, Yao HH-C. Somatic cell fate maintenance in mouse fetal testes via autocrine/paracrine action of AMH and activin B. *Nat Commun* 2022; **13**:4130.
74. Inhibin, activin, follistatin and FSH serum levels and testicular production are highly modulated during the first spermatogenic wave in mice. *Reproduction* 2008; **136**:345–359.
75. Soffientini U, Rebourcet D, Abel MH, Lee S, Hamilton G, Fowler PA, Smith LB, O'Shaughnessy PJ. Identification of Sertoli cell-specific transcripts in the mouse testis and the role of FSH and androgen in the control of Sertoli cell activity. *BMC Genomics* 2017; **18**:972.
76. Villalpando I, Lira E, Medina G, Garcia-Garcia E, Echeverria O. Insulin-like growth factor 1 is expressed in mouse developing testis and regulates somatic cell proliferation. *Exp Biol Med (Maywood)* 2008; **233**:419–426.
77. Magueresse-Battistoni BL. Serine proteases and serine protease inhibitors in testicular physiology: the plasminogen activation system. *Reproduction* 2007; **134**:721–729.
78. Le Magueresse-Battistoni B, Pernod G, Sigillo F, Kolodié L, Benahmed M. Plasminogen activator Inhibitor-1 is expressed in cultured rat Sertoli Cells1. *Biol Reprod* 1998; **59**:591–598.
79. Yamamiya K, Li X, Nabeka H, Khan S, Khan F, Wakisaka H, Saito S, Hamada F, Matsuda S. Tracking of Prosaposin, a Saposin precursor, in rat testis. *J Histochem Cytochem* 2023; **71**:537–554.
80. Morales CR, Hay N, El-Alfy M, Zhao Q. Distribution of Mouse Sulfated Glycoprotein-1 (Prosaposin) in the Testis and Other Tissues. *J Androl* 1998; **19**:156–164.
81. Chassot A-A, Le Rolle M, Jolivet G, Stevant I, Guigonis J-M, Da Silva F, Nef S, Pailhoux E, Schedl A, Ghyselinck NB, Chaboissier M-C. Retinoic acid synthesis by ALDH1A proteins is dispensable for meiosis initiation in the mouse fetal ovary. *Sci Adv*n.d. **6**:eaaz1261.
82. Arnold SLM, Kent T, Hogarth CA, Griswold MD, Amory JK, Isoherranen N. Pharmacological inhibition of ALDH1A in mice decreases all-trans retinoic acid concentrations in a tissue specific manner. *Biochem Pharmacol* 2015; **95**:177–192.
83. Hogarth CA, Arnold S, Kent T, Mitchell D, Isoherranen N, Griswold MD. Processive pulses of retinoic acid propel asynchronous and continuous murine sperm production. *Biol Reprod* 2015; **92**:37.
84. Farjo KM, Moiseyev G, Nikolaeva O, Sandell LL, Trainor PA, Ma J. RDH10 is the primary enzyme responsible for the first step of embryonic vitamin a metabolism and retinoic acid synthesis. *Dev Biol* 2011; **357**:347–355.
85. Bowles J, Feng C-W, Knight D, Smith CA, Roeszler KN, Bagheri-Fam S, Harley VR, Sinclair AH, Koopman P. Male-specific expression of Aldh1a1 in mouse and chicken fetal testes: implications for retinoid balance in gonad development. *Dev Dyn* 2009; **238**:2073–2080.
86. Hofmann M-C, Mcbeath E. Sertoli cell-germ cell interactions within the niche: paracrine and Juxtacrine molecular communications. *Front Endocrinol* 2022; **13**:13.
87. Bellvé AR, Cavicchia JC, Millette CF, O'Brien DA, Bhatnagar YM, Dym M. Spermatogenic cells of the prepuberal mouse. Isolation and morphological characterization. *J Cell Biol* 1977; **74**:68–85.
88. Chen G, Ning B, Shi T. Single-cell RNA-Seq technologies and related computational data analysis. *Front Genet* 2019; **10**:317.
89. Washburn RL, Hibler T, Kaur G, Dufour JM. Sertoli cell immune regulation: a double-edged sword. *Front Immunol* 2022; **13**:913502.
90. Washburn RL, Hibler T, Thompson LA, Kaur G, Dufour JM. Therapeutic application of Sertoli cells for treatment of various diseases. *Semin Cell Dev Biol* 2022; **121**:10–23.
91. Wang J, Wreford NGM, Lan HY, Atkins R, Hedger MP. Leukocyte populations of the adult rat testis following removal of the Leydig cells by treatment with ethane Dimethane sulfonate and subcutaneous testosterone Implants1. *Biol Reprod* 1994; **51**:551–561.
92. Lymar ES, Clark AM, Reeves R, Griswold MD. Clusterin gene in rat Sertoli cells is regulated by a Core-enhancer element. *Biol Reprod* 2000; **63**:1341–1351.
93. Naponelli V, Bettuzzi S. Chapter 32 - Clusterin. In: Barnum S, Schein T (eds.), *The Complement FactsBook (Second Edition)*. Cambridge: Academic Press; 2018: 341–349.
94. Endo T, Romer KA, Anderson EL, Baltus AE, de Rooij DG, Page DC. Periodic retinoic acid–STRA8 signaling intersects with periodic germ-cell competencies to regulate spermatogenesis. *PNAS* 2015; **112**:E2347–E2356.
95. La Sala G, Marazziti D, Di Pietro C, Golini E, Matteoni R, Tocchini-Valentini GP. Modulation of Dhh signaling and altered Sertoli cell function in mice lacking the GPR37-prosaposin receptor. *FASEB J* 2015; **29**:2059–2069.
96. Mahyari E, Guo J, Lima AC, Lewinsohn DP, Stendahl AM, Vigh-Conrad KA, Nie X, Nagirnaja L, Rockweiler NB, Carrell DT, Hotaling JM, Aston KI, *et al.* Comparative single-cell analysis of biopsies clarifies pathogenic mechanisms in Klinefelter syndrome. *The American Journal of Human Genetics* 2021; **108**:1924–1945.
97. Bu T, Wang L, Wu X, Li L, Mao B, Wong CKC, Perrotta A, Silvestrini B, Sun F, Cheng CY. A laminin-based local regulatory network in the testis that supports spermatogenesis. *Semin Cell Dev Biol* 2022; **121**:40–52.
98. Harvey SJ, Perry J, Zheng K, Chen D, Sado Y, Jefferson B, Ninomiya Y, Jacobs R, Hudson BG, Thorner PS. Sequential expression of type IV Collagen networks: testis as a model and relevance to spermatogenesis. *Am J Pathol* 2006; **168**:1587–1597.
99. Sona C, Yeh Y-T, Patsalos A, Halasz L, Yan X, Kononenko NL, Nagy L, Poy MN. Evidence of islet CADM1-mediated immune cell interactions during human type 1 diabetes. *JCI Insight* n.d.; **7**:e153136.
100. Jiang X, Ma T, Zhang Y, Zhang H, Yin S, Zheng W, Wang L, Wang Z, Khan M, Sheikh SW, Bukhari I, Iqbal F, *et al.* Specific deletion of Cdh2 in Sertoli cells leads to altered meiotic progression and subfertility of Mice1. *Biol Reprod* 2015; **92**:1–12.
101. Nguyen TMD. Adiponectin: role in physiology and pathophysiology. *Int J Prev Med* 2020; **11**:136.
102. Feng S, Isayev O, Werner J, Bazhin AV. CD96 as a potential immune regulator in cancers. *Int J Mol Sci* 2023; **24**:1303.
103. Lee GR, Shaefi S, Otterbein LE. HO-1 and CD39: it takes two to protect the realm. *Front Immunol* 2019; **10**:3389.
104. Zhang C, Hu C, Su K, Wang K, Du X, Xing B, Liu X. The integrative analysis of thrombospondin family genes in pan-cancer

reveals that THBS2 facilitates gastrointestinal cancer metastasis. *J Oncol* 2021; **2021**e4405491:1–19.
105. Grandis M, Vigo T, Passalacqua M, Jain M, Scazzola S, La Padula V, Brucal M, Benvenuto F, Nobbio L, Cadoni A, Mancardi GL, Kamholz J, *et al*. Different cellular and molecular mechanisms for early and late-onset myelin protein zero mutations. *Hum Mol Genet* 2008; **17**:1877–1889.
106. Calandra T, Roger T. Macrophage migration inhibitory factor: a regulator of innate immunity. *Nat Rev Immunol* 2003; **3**: 791–800.
107. van der Horst EH, Frank BT, Chinn L, Coxon A, Li S, Polesso F, Slavin A, Ruefli-Brasse A, Wesche H. The growth factor Midkine antagonizes VEGF Signaling In vitro and In vivo. *Neoplasia* 2008; **10**:340–IN3.